

On the rotational stability of nonspherical particles driven by the radiation torque

Ferdinando Borghese, Paolo Denti, Rosalba Saija, Maria Antonia Iatì

*Dipartimento di Fisica della Materia e Tecnologie Fisiche Avanzate,
Università di Messina, Salita Sperone 31, 98166 Messina, Italy*

borghese@ortica.unime.it

Abstract: We calculate the radiation torque exerted by a monochromatic plane wave, either unpolarized or linearly polarized, on aggregates of spheres and investigate the stability of the resulting rotational motion. In fact, neglecting any braking momenta we calculate the component of the electromagnetic torque orthogonal to the principal axis of maximum moment of inertia through the center of mass (transverse torque), as a function of the direction of propagation of the incident field. The aggregates we study are composed of homogeneous spheres, possibly of different materials. The electromagnetic torque is calculated through the transition matrix approach along the lines of the theory reported in our recent paper [F. Borghese, P. Denti, R. Saija and M. A. Iatì, *Opt. Express* **14**, 9508 (2006)]. When the transverse component of the electromagnetic torque is small or vanishes the rotational motion driven by the component along the principal axis of inertia may be nearly stable.

© 2007 Optical Society of America

OCIS codes: (290.0290) Scattering, (260.2110) Electromagnetic theory, (260.2160) Energy transfer, (999.9999) Radiation Torque.

References and links

1. J. D. Jackson, *Classical electrodynamics*, 2d edition (Wiley, New York, 1975).
2. M. E. J. Friese, T.A. Nieminen, N. R. Heckenberg and H. Rubinsztein-Dunlop, "Optical alignment and spinning of laser-trapped microscopic particles," *Nature* **394**, 348-349 (1998).
3. M. E. J. Friese, T.A. Nieminen, N. R. Heckenberg and H. Rubinsztein-Dunlop, "Erratum: Optical alignment and spinning of laser-trapped microscopic particles," *Nature* **395**, 621 (1998).
4. P. Galajda and P. Ormos, "Rotation of microscopic propellers in laser tweezers," *J. Opt. B: Quantum Semiclass. Opt.* **4**, S78-S81 (2002).
5. E. M. Purcell, "Suprathermal rotation of interstellar grains," *Astrophys. J.* **231**, 404-416 (1979).
6. A. Lazarian, "Physics of grain alignment," in *Cosmic evolution and galaxy formation*, AIP Conference series **3**, (1999).
7. B. T. Draine and J. C. Weingartner, "Radiative torques on interstellar grains. I. Superthermal spin-up," *Astrophys. J.* **470**, 551-565 (1996).
8. B. T. Draine and J. C. Weingartner, "Radiative torques on interstellar grains. II. Grain alignment," *Astrophys. J.* **480**, 633-646 (1997).
9. E. M. Purcell and C. R. Pennypacker, "Scattering and absorption of light by nonspherical dielectric grains," *Astrophys. J.* **186**, 705-714 (1973).
10. B. T. Draine and P. J. Flatau, "Discrete dipole approximation for scattering calculations," *J. Opt. Soc. Am. A* **11**, 1491-1499 (1994).
11. P. C. Waterman, "Symmetry, unitarity and geometry in electromagnetic scattering," *Phys. Rev. D* **4**, 825-839 (1971).

12. P. L. Marston and J. H. Crichton, "Radiation torque on a sphere caused by a circularly-polarized electromagnetic wave," *Phys. Rev. A* **30**, 2508–2516 (1984).
13. F. J. García de Abajo, "Electromagnetic forces and torques in nanoparticles irradiated by plane waves," *J. Quant. Spectrosc. Radiat. Transfer* **89**, 3–9 (2004).
14. F. J. García de Abajo, "Momentum transfer to small particles by passing electron beams," *Phys. Rev. B* **70**, 115422 (2004).
15. F. Borghese, P. Denti, R. Saija and M. A. Iatì, "Radiation torque on nonspherical particles in the transition matrix formalism," *Opt. Express* **14**, 9508–9521 (2006).
16. F. Borghese, P. Denti and R. Saija, *Scattering from model nonspherical particles*, 2nd edition (Springer, Berlin, 2007).
17. R. Saija, M. A. Iatì, P. Denti, F. Borghese, A. Giusto and O. I. Sindoni, "Efficient light-scattering calculations for aggregates of large spheres," *Appl. Opt.* **42**, 2785–2793 (2003).
18. R. Saija, M. A. Iatì, F. Borghese, P. Denti, S. Aiello and C. Cecchi-Pestellini, "Beyond Mie theory: the transition matrix approach in interstellar dust modeling," *Astrophys. J.* **559**, 993–1004 (2001).
19. Y.-L. Xu, "Electromagnetic scattering by an aggregate of spheres," *Appl. Opt.* **34**, 4573–4588 (1995).
20. W. C. Chew, *Waves and fields in inhomogeneous media*, IEEE Press Series on Electromagnetic Waves (Institute of Electrical and Electronic Engineers, Piscataway, N.J., 1990).
21. F. Borghese, P. Denti, R. Saija and M. A. Iatì, "Radiation torque on nonspherical particles in the transition matrix formalism: erratum," *Opt. Express* **15**, 6946 (2007).
22. The Erratum to Ref. [16] can be found at <http://dfmtfa.unime.it/profs/borghese/ferdinandoborghese.html>.
23. M. I. Mishchenko, "Radiation force caused by scattering, absorption and emission of light by nonspherical particles," *J. Quant. Spectrosc. Radiat. Transfer* **70**, 811–816 (2001).
24. E. M. Rose, *Elementary theory of angular momentum*, (Wiley, New York, 1956).
25. H. Goldstein, C. Poole and J. Safko, *Classical Mechanics*, 3d edition (Addison-Wesley, Reading, Mass., 2002).
26. B. T. Draine and H. M. Lee, "Optical properties of interstellar graphite and silicate grains," *Astrophys. J.* **285**, 89–108 (1984).
27. P. H. Berning, G. Hass and P. R. Madden, "Reflectance-increasing coatings for the vacuum ultraviolet and their applications," *J. Opt. Soc. Am.* **50**, 586–597 (1960).
28. U. Kreibig, "Electronic properties of small silver particles: the optical constants and their temperature dependence," *J. Phys. F: Metal Phys.* **4**, 999–1014 (1974).
29. G. Wurm and M. Schneider, "Coagulation as a unifying element for interstellar polarization," *Astrophys. J.* **567**, 370–375 (2002).

1. Introduction

The conservation of the angular momentum for the combined system of radiation field and particles implies that an electromagnetic wave impinging on a particle exerts a mechanical torque on the latter [1]. This fact has found useful applications in the manipulation of micro- and nanoparticles [2, 3]. For instance, the torque experienced by propeller-shaped particles embedded into a viscous fluid and trapped by optical tweezers induces rotations that through microrheologic studies give information on the properties both of the fluid and of the particles themselves [4]. The electromagnetic torque is also of interest for astrophysicists, because, according to the suggestion of Purcell [5], it is considered as a relevant agent for the alignment of cosmic dust grains, that is required to explain the linearly polarized component of the starlight [6].

The actual evaluation of the radiation torque requires calculating the radiation field in the presence of the particles. For instance, Draine and Weingartner [7, 8] calculated through the discrete dipole approximation (DDA) [9, 10] the field scattered by model cosmic grains and the torque experienced by the latter. Unfortunately, due to the large amount of calculations required by the DDA, it is not surprising that the above authors dealt with a few simple model particles only.

The computational effort is more sustainable, even for particles with a complex structure, by using the multipole expansion of the field in the framework of the transition matrix approach [11]. As far as we know, the first complete solution to the problem of radiation torque in terms of multipole fields is due to Marston and Crichton [12] who dealt with the torque exerted by an elliptically polarized plane wave on a homogeneous sphere. More recently, the multipole field expansion has been exploited by de Abajo [13, 14] to calculate the radiation torque on model

nonspherical particles. The transition matrix approach was further extended by the present authors to the case of particles shaped as aggregates of spherical scatterers [15, 16, 21, 22], the stability of whose induced rotations has also been discussed to some extent. Our main conclusion was that when a circularly polarized plane wave impinges on a cluster composed of identical spheres along one of the principal axes of inertia through the center of mass the induced rotations are nearly stable even when the cluster lacks any symmetry.

Nevertheless, in laboratory experiments linearly polarized light is mostly used, whereas in an astrophysical environment the light is mainly unpolarized. Moreover, the rotations driven by radiation torque may be unstable, whatever the polarization, when the dielectric properties of the aggregated spheres are not equal to each other. In fact, the mechanical properties of the clusters, such as the moment of inertia tensor, are determined by the distribution of the masses, whereas the electromagnetic torque is determined by the distribution of the dielectric properties, mainly by the absorptivity of the component spheres. Therefore, the purpose of this paper is to report a study of the rotational stability of clusters composed of spheres with different dielectric properties, when the electromagnetic torque is due to an unpolarized plane wave or to a linearly polarized plane wave.

Indeed, the problem of rotational stability has already been faced by Draine and Weingartner in an astrophysical context by solving numerically the equations of rotational motion of a particle of known morphology and refractive index [8]. Here, we adopt a simpler approach: we calculate the electromagnetic torque exerted on the particles by a plane wave. Then, we calculate the component of the torque in a plane orthogonal to the central axis of maximum moment of inertia as a function of the direction of incidence of the incoming radiation. It is intuitive that a nearly stable rotation around this axis cannot occur unless the transverse torque is small.

2. Radiation torque

In this section we report the essentials of the theory of the torque exerted by a monochromatic plane wave on aggregated spheres. The interested reader is referred to our recent paper [15] and to Ref. [16] for further details.

We assume that the particle of interest is embedded into a homogeneous medium of refractive index n . Then, a monochromatic wave exerts a torque on the particle given by

$$\vec{\Gamma}_{\text{rad}} = - \oint \hat{\mathbf{n}} \cdot \langle \mathbf{T}_M \rangle \times \mathbf{r} dS, \quad (1)$$

where $\hat{\mathbf{n}}$ is the unit outward normal to an arbitrarily chosen closed surface S that surrounds the particle and

$$\langle \mathbf{T}_M \rangle = \frac{1}{8\pi} \text{Re} [n^2 \mathbf{E} \otimes \mathbf{E}^* + \mathbf{B} \otimes \mathbf{B}^* - \frac{1}{2} (n^2 \mathbf{E} \cdot \mathbf{E}^* + \mathbf{B} \cdot \mathbf{B}^*) \mathbf{l}] \quad (2)$$

is the time averaged Maxwell stress tensor, \mathbf{l} being the unit dyadic. Of course, in Eq. (2)

$$\mathbf{E} = \mathbf{E}_I + \mathbf{E}_S, \quad \mathbf{B} = \mathbf{B}_I + \mathbf{B}_S,$$

i.e., \mathbf{E} and \mathbf{B} are the superposition of the incident and of the scattered fields.

We found convenient to choose the integration surface S to be a sphere of arbitrary radius with its center within the particle, so that Eq. (1) becomes

$$\vec{\Gamma}_{\text{rad}} = -r^3 \int_{\Omega} \hat{\mathbf{r}} \cdot \langle \mathbf{T}_M \rangle \times \hat{\mathbf{r}} d\Omega. \quad (3)$$

Since $\hat{\mathbf{r}} \cdot \mathbf{l} \times \hat{\mathbf{r}} = 0$, the last two terms in Eq. (2) give no contribution to the integral, and by choosing the radius of the integration sphere to be large, possibly infinite, we can resort to the

asymptotic expression of the fields. Nevertheless, it should be borne in mind that using the customary far zone expression of the scattered field in terms of the scattering amplitude

$$\mathbf{E}_S = \frac{\exp(ikr)}{r} \mathbf{f}(\hat{\mathbf{k}}_S, \hat{\mathbf{k}}_I)$$

yields a vanishing result because $\hat{\mathbf{r}} \cdot \mathbf{f} = 0$ [23]. Therefore, the correct procedure requires that, after solving the problem of scattering, the fields be expanded for large r and all terms that give contributions of order $1/r^3$ to the integrand in Eq. (3) be retained.

Since the polarization of the field is relevant, we introduce a pair of mutually orthogonal unit vectors, say $\hat{\mathbf{u}}_\eta$, such that

$$\hat{\mathbf{u}}_1 \times \hat{\mathbf{u}}_2 = \hat{\mathbf{k}}_I,$$

where $\hat{\mathbf{k}}_I$ is the direction of the propagation of the incident plane wave. Note that the vectors $\hat{\mathbf{u}}_\eta$ may be either real (linear polarization basis) or complex (circular polarization basis). In case the linear polarization basis is used the subscripts $\eta = 1, 2$ denote polarization parallel and perpendicular to a fixed plane of reference through $\hat{\mathbf{k}}_I$, respectively, whereas, when the circular basis is used, $\eta = 1, 2$ denote left and right polarization, respectively.

Both the incident and the scattered field are expanded in a series of vector multipole fields [16]. Accordingly,

$$\mathbf{E}_I = \sum_{\eta} E_{0\eta} \hat{\mathbf{u}}_{\eta} \exp(i\mathbf{k} \cdot \mathbf{r}) = \sum_{\eta} E_{0\eta} \sum_{plm} \mathbf{J}_{lm}^{(p)}(\mathbf{r}, k) W_{\eta lm}^{(p)}, \quad (4a)$$

$$\mathbf{E}_S = \sum_{\eta} E_{0\eta} \sum_{plm} \mathbf{H}_{lm}^{(p)}(\mathbf{r}, k) A_{\eta lm}^{(p)}, \quad (4b)$$

where $k = nk_v$, with $k_v = \omega/c$, is the propagation constant of the incident plane wave. We also define the multipole fields in (4a) according to

$$\mathbf{J}_{lm}^{(1)}(\mathbf{r}, k) = j_l(kr) \mathbf{X}_{lm}(\hat{\mathbf{r}}), \quad \mathbf{J}_{lm}^{(2)}(\mathbf{r}, k) = \frac{1}{k} \nabla \times \mathbf{J}_{lm}^{(1)}(\mathbf{r}, k), \quad (5)$$

where $\mathbf{X}_{lm}(\hat{\mathbf{r}})$ denotes vector spherical harmonics [1]. The multipole fields $\mathbf{H}_{lm}^{(p)}(\mathbf{r}, k)$ in (4b) are identical to the $\mathbf{J}_{lm}^{(p)}(\mathbf{r}, k)$ fields (5) except for the substitution of the spherical Hankel functions of the first kind $h_l(kr)$ in place of the spherical Bessel functions $j_l(kr)$. The (known) multipole amplitudes of the incident field $W_{\eta lm}^{(p)}$ are defined in [15, 16], whereas the amplitudes of the scattered field $A_{\eta lm}^{(p)}$ are calculated by imposing the customary boundary conditions across the surface of the particle. The amplitudes $A_{\eta lm}^{(p)}$ bear the index η to recall the polarization of the incident field, and are related to the $W_{\eta lm}^{(p)}$ by [16]

$$A_{\eta lm}^{(p)} = \sum_{p'l'm'} \mathcal{S}_{lm'l'm'}^{(pp')} W_{\eta l'm'}^{(p')}. \quad (6)$$

Equation (6) defines the elements $\mathcal{S}_{lm'l'm'}^{(pp')}$ of the so-called transition matrix of the particle [11]. Now, the particles the present study is going to deal with either actually are, or can be modeled as aggregates of spheres. We calculate $\mathcal{S}_{lm'l'm'}^{(pp')}$ for such aggregates always starting with the inversion of the matrix of the linear system that is obtained by imposing to the fields the boundary conditions across each of the spherical surfaces [17, 18]. The order of the matrix to be inverted is $2Nl_M(l_M + 2)$, where N is the number of the spheres of the aggregate and l_M is the maximum value of l to be retained in the multipole expansions of the fields (4) in order to

get convergence for the quantities of interest. The convergence of such kind of calculations is studied in Ref. [17]. A comprehensive treatment of all the abovementioned topics related to the calculation of the transition matrix can be found in Ref. [16]. Anyway, we are well aware that other procedures for calculating the transition matrix elements have been devised, such as the iterative procedures of Xu [19] and of Chew [20], but we never used them for reasons that are fully expounded in Ref. [17].

Let us now define the vector $\vec{\Gamma}$ such that

$$\vec{\Gamma}_{\text{Rad}} = \text{Re}(\vec{\Gamma})$$

and in terms of whose spherical components [24] the cartesian components of $\vec{\Gamma}_{\text{Rad}}$ read

$$\Gamma_{\text{Rad},x} = \text{Re}\left[\frac{1}{\sqrt{2}}(\Gamma_{-1} - \Gamma_1)\right], \quad \Gamma_{\text{Rad},y} = \text{Re}\left[\frac{i}{\sqrt{2}}(\Gamma_{-1} + \Gamma_1)\right], \quad \Gamma_{\text{Rad},z} = \text{Re}(\Gamma_0), \quad (7)$$

where

$$\Gamma_{\mu} = \sum_{\eta\bar{\eta}} I_{I\bar{\eta}\eta} \Gamma_{\mu;\bar{\eta}\eta}, \quad (8)$$

with $I_{I\bar{\eta}\eta} = E_{0\bar{\eta}}^* E_{0\eta}$. At this stage, the procedure fully expounded in [15] and [16] yields for $\Gamma_{\mu;\bar{\eta}\eta}$ the expression

$$\Gamma_{\mu;\bar{\eta}\eta} = \Gamma_{\mu;\bar{\eta}\eta}^{(\text{ext})} - \Gamma_{\mu;\bar{\eta}\eta}^{(\text{sca})}, \quad (9)$$

where

$$\Gamma_{\mu;\bar{\eta}\eta}^{(\text{ext})} = c_{\Gamma} \sum_{plm} s_{\mu;lm} W_{I\eta l, m-\mu}^{(p)} A_{\bar{\eta}lm}^{(p)*}, \quad (10)$$

whereas the quantities $\Gamma_{\mu;\bar{\eta}\eta}^{(\text{sca})}$ are identical to the $\Gamma_{\mu;\bar{\eta}\eta}^{(\text{ext})}$ above, except for the substitution of $A_{\eta lm}^{(p)}$ in place of $W_{I\eta lm}^{(p)}$ and for the change of the sign. In Eq. (10) we define $c_{\Gamma} = n^2/8\pi k^3$ and

$$s_{-1;lm} = -\sqrt{\frac{(l-m)(l+1+m)}{2}}, \quad s_{0;lm} = -m, \quad s_{1;lm} = \sqrt{\frac{(l+m)(l+1-m)}{2}}. \quad (11)$$

In [15] we demonstrated that Eqs. (7)–(11), when applied to a homogeneous sphere, reproduce the results of Marston and Crichton [12].

Let us assume that the particles we consider are freely rotating at a temperature T . Then, their angular velocity is given by

$$\omega_T = \sqrt{k_B T / I},$$

where k_B is the Boltzman constant and I is the moment of inertia around the axis of rotation; $\omega_T \approx 10^4 \text{ sec}^{-1}$ at $T = 100\text{K}$ for the particles we deal with. Therefore, according to the suggestion of Draine and Weingartner [7, 8], it is reasonable to assume that at such an angular velocity the particles should experience only a torque averaged over a complete rotation. In Ref. [15] we explained as such average of the radiation torque can be calculated through an analytic procedure, to which we will refer as *axial averaging*. The relevant formulas are

$$\begin{aligned} \langle \Gamma_{\mu;\bar{\eta}\eta}^{(\text{ext})} \rangle &= c_{\Gamma} \sum_{plm} s_{\mu;lm} \sum_{\bar{p}\bar{l}} W_{I\eta l, m-\mu}^{(p)} \bar{\mathcal{F}}_{l\bar{m}l\bar{m}}^{(p\bar{p})*} W_{I\bar{\eta}l\bar{m}}^{(\bar{p})}, \\ \langle \Gamma_{\mu;\bar{\eta}\eta}^{(\text{sca})} \rangle &= -c_{\Gamma} \sum_{plm} s_{\mu;lm} \sum_{\bar{p}\bar{p}'} \sum_{\bar{l}\bar{l}'} \sum_{m'} \bar{\mathcal{F}}_{l, m-\mu, \bar{l}, m'-\mu}^{(p\bar{p})} W_{I\eta l, m'-\mu}^{(\bar{p})} \bar{\mathcal{F}}_{l\bar{m}'\bar{m}'}^{(p\bar{p}')*} W_{I\bar{\eta}l'\bar{m}'}^{(\bar{p}')}, \end{aligned} \quad (12)$$

where the bar over the elements of the transition matrix indicates that they are calculated in a frame of reference fixed to the cluster. We stress that the formulas corresponding to (12) reported in Refs. [15, 16] were written with wrong indices but that the calculations were performed using the correct expressions above [21, 22].

3. Radiation torque on aggregated spheres

Since in this paper we focus on the stability of the rotation driven by the radiation torque, we resolved to neglect any other torque. For instance, we neglect the frictional torque due to the surrounding medium and the braking torques due to magnetic fields. In the present case, we assumed that the particles are embedded in vacuo and, accordingly, we set $n = 1$. We stress, however, that the mechanical effects of the embedding medium as well as those of magnetic fields should be taken into account when a realistic description of the dynamics of the particles is required. In this respect let us recall that a steady rotation of a free particle can occur only around one of the principal axes of inertia through the center of mass and that in case braking momenta are applied a stable rotation may occur only around the principal axis of maximum moment of inertia [25].

The quantity which we actually calculated is the adimensional vector

$$\mathbf{T}_\eta = \frac{8\pi k}{I_1 \sigma_{T\eta}} \vec{\Gamma}_{\text{Rad}\eta},$$

where $\vec{\Gamma}_{\text{Rad}\eta}$ is the radiation torque calculated for incident light with polarization η and $\sigma_{T\eta}$ is the extinction cross section of the particle concerned for polarization η . All the aggregates that we consider hereafter are composed of five spherical homogeneous scatterers whose space arrangement is chosen so that no symmetry is present, but each of the aggregated spheres is

Table 1. Densities in g/cm^3 and dielectric constants at $\lambda = 380\text{nm}$ of the materials that compose the clusters

	ρ	ϵ_r	ϵ_i
Si	3.30	3.012	0.1005
C	1.85	2.773	2.766
Al	2.70	-16.49	2.856
Ag	10.49	-3.2	1.65

Table 2. Composition of the clusters and radii of the component spheres in nm

A	4 Si	$b_{\text{Si}}=50$	1 Al	$b_{\text{Al}}=50$
B	4 C	$b_{\text{C}}=50$	1 Al	$b_{\text{Al}}=50$
C	4 C	$b_{\text{C}}=50$	1 Ag	$b_{\text{Ag}}=50$
D	4 C	$b_{\text{C}}=50$	1 Ag	$b_{\text{Ag}}=28$

in contact with at least one other sphere of the aggregate. The materials we chose to build the aggregates under study are the so-called astronomical silicates and amorphous carbon [26] to which we added aluminum [27] and silver [28] because their density and/or dielectric function are the most different from those of the other materials. The composition of the aggregates is given in Table 2 where the radii of the component spheres are also reported. In this respect we stress that in cluster D the radius of the sphere of Ag is 28 nm, so that its mass equals that of a sphere of carbon. Table 3 reports, for all the clusters we investigated, the coordinates in nm of the centers of the spheres, with respect to a frame of reference with origin in the center of

Table 3. Coordinates of the centers of the spheres (in nm) with respect to the frame of reference with origin at the center of mass. The principal moments of inertia are also given in $\text{g} \cdot \text{cm}^2 \times 10^{28}$

Cluster A						
x	37.945	37.771	-52.580	-141.093	124.855	$I_{xx} = 3.056$
y	102.858	2.876	-37.061	-3.717	-46.254	$I_{yy} = 8.011$
z	-3.041	-1.160	-19.663	14.312	9.000	$I_{zz} = 10.000$
Cluster B						
x	41.771	32.317	-61.312	-146.417	114.447	$I_{xx} = 2.336$
y	87.298	-12.249	-43.445	-2.367	-69.346	$I_{yy} = 4.652$
z	-1.741	-0.860	-19.856	14.357	8.901	$I_{zz} = 6.327$
Cluster C						
x	-45.118	12.972	109.499	162.765	-29.401	$I_{xx} = 4.013$
y	-30.826	50.570	30.477	-47.477	141.221	$I_{yy} = 5.949$
z	-0.457	-0.563	-20.447	14.400	8.802	$I_{zz} = 8.892$
Cluster D						
x	36.207	36.414	-53.759	-142.421	123.711	$I_{xx} = 1.456$
y	81.736	3.757	-36.662	-3.545	-44.941	$I_{yy} = 4.465$
z	-3.983	-1.148	-19.471	14.447	9.252	$I_{zz} = 5.372$

mass and the axes along the principal axes of inertia, the z axis being chosen along the axis of maximum moment of inertia. We also report the values of the principal moments of inertia.

All our calculations were performed using $l_M = 12$ in order to ensure the complete coverage of the quantities of interest [16, 17].

The results of our calculations for the transverse component of the radiation torque on clusters A–D are reported in Figs. 1–4, both for unpolarized light and for linearly polarized light. More precisely, panels (a) of each figure show a sketch of the geometry whereas panels (b) report $T_{\perp} = (T_x^2 + T_y^2)^{1/2}$ for unpolarized light and panels (c) and (d) for linearly polarized light with $\eta = 1, 2$, respectively, as a function of the direction of incidence of the incoming radiation, given by the polar angles ϑ_I and φ_I . The plane of reference for the linear polarization is the meridional plane defined by \mathbf{k}_I and the z axis.

First, we note that the transverse component T_{\perp} does not vanish for incidence either parallel ($\vartheta_I = 0^\circ$) or antiparallel ($\vartheta_I = 180^\circ$) to the axis of maximum moment of inertia, and that, in linear polarization, it is not constant as φ_I varies. On the other hand, all the graphs show a minimum for some value of ϑ_I . In our opinion, the first feature stems from the mismatch between the distribution of the masses and the distribution of the dielectric properties. In fact, we already stressed in Ref. [16] that the vanishing of the transverse torque can occur only when the aggregate has a cylindrical symmetry axis coincident with the axis of rotation and the incident wavevector is along this axis. In turn, the existence of the minima for $\vartheta_I \neq 0$ suggests that the rotation may be stable when the incidence is not along a principal axis of inertia.

4. Axial averages

The graphs presented in Sect. 3 give the dependence of the transverse torque T_{\perp} as a function of the direction of incidence of the field. As regards the dependence on φ_I , it may be useful to remark that it gives information on the behaviour of T_{\perp} as a function of the orientation of the

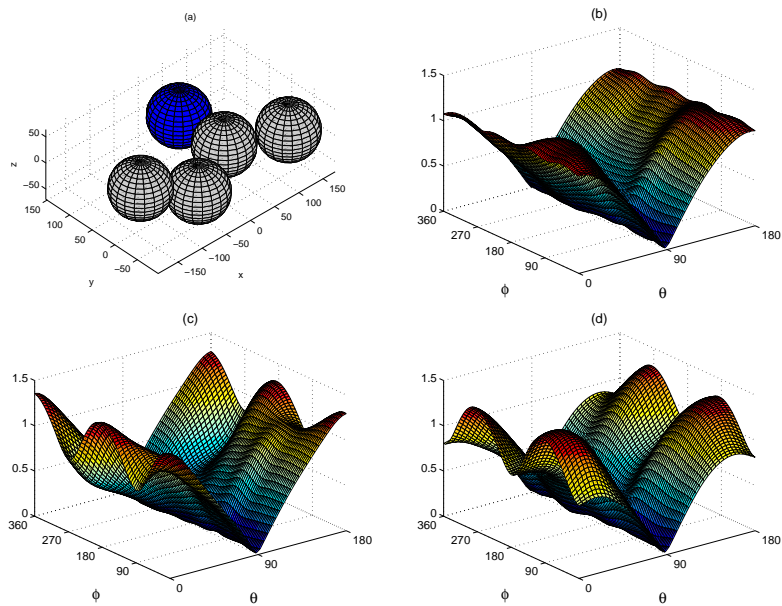


Fig. 1. T_{\perp} as a function of the angles of incidence ϑ_1 and φ_1 for cluster A of four spheres of astronomical silicates (gray) and one sphere of aluminum (blue) whose geometry is shown in (a). The light is unpolarized in (b), and linearly polarized with $\eta = 1, 2$ in (c) and (d), respectively.

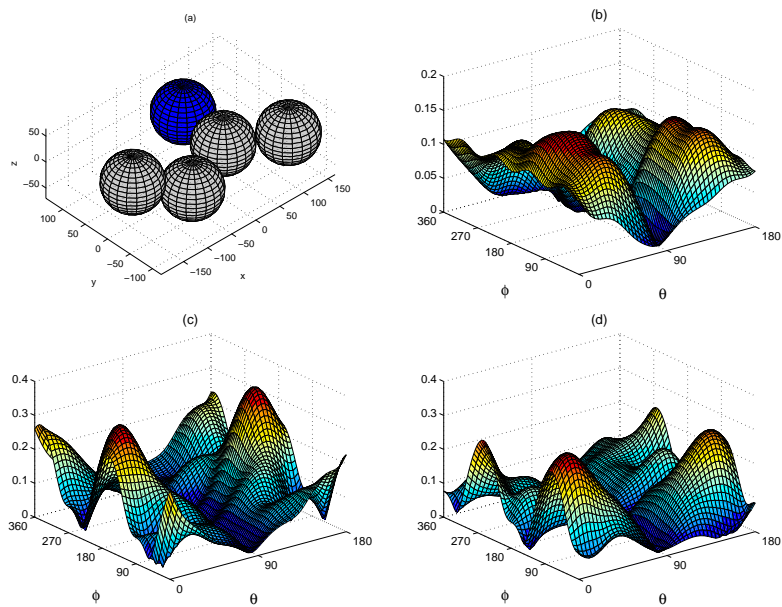


Fig. 2. Same of Fig. 1 for cluster B of four spheres of amorphous carbon (gray) and one sphere of aluminum (blue) whose geometry is shown in (a).

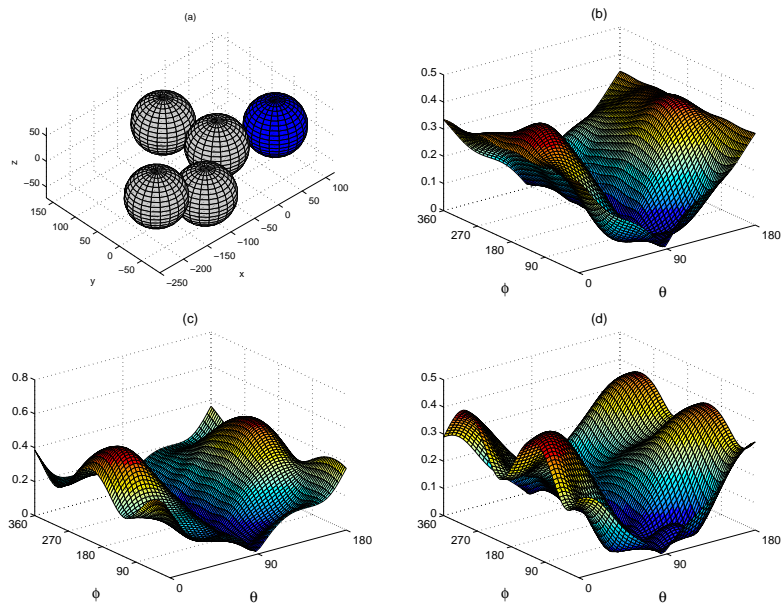


Fig. 3. Same of Fig. 1 for cluster C of four spheres of amorphous carbon (gray) and one sphere of silver (blue) whose geometry is shown in (a).

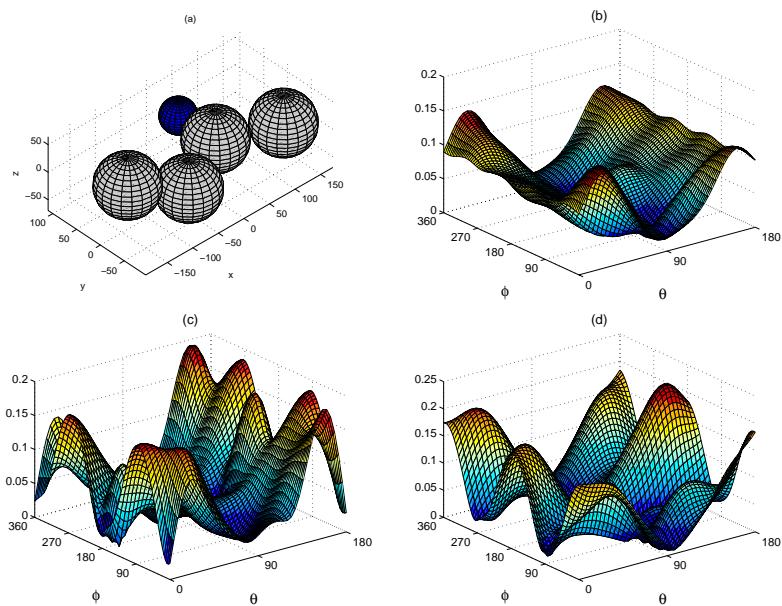


Fig. 4. Same of Fig. 1 for cluster D of four spheres of amorphous carbon (gray) and one sphere of silver (blue) whose geometry is shown in (a). The radius of the silver sphere is 28 nm so that its mass is equal to the mass of a sphere of carbon.

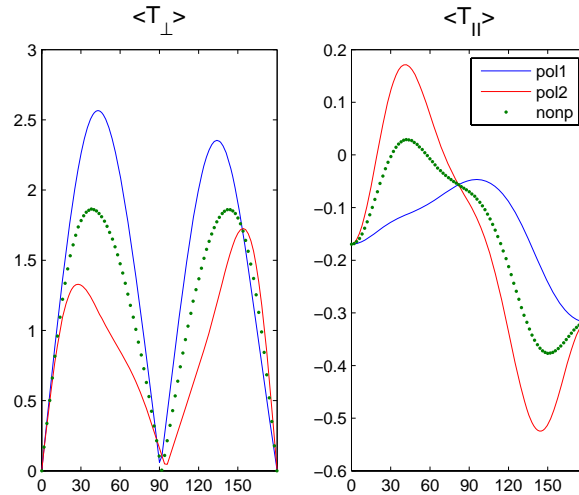


Fig. 5. Axial averages $\langle T_{\perp} \rangle$ and $\langle T_{\parallel} \rangle$ as a function of ϑ_1 for cluster A.

particle around the axis of maximum moment of inertia (z axis). Therefore, provided the particle is rotating around the z axis with a sufficiently high speed, it makes sense to consider the axial averages around the axis of rotation. Accordingly, in Figs. 5–8 we present the axial averages $\langle T_{\perp} \rangle = \sqrt{\langle T_x \rangle^2 + \langle T_y \rangle^2}$ and $\langle T_z \rangle$ for the aggregates considered so far, both for unpolarized light and for linearly polarized light with $\eta = 1, 2$. $\langle T_z \rangle$ gives the torque that actually drives the rotational motion of the aggregate around the z axis.

We first note that in all the cases we considered the transverse torque vanishes for $\vartheta_1 = 0^\circ$ and for $\vartheta_1 = 180^\circ$, i.e., for incidence along the axis of maximum moment of inertia. For this incidence $\langle T_z \rangle$ never vanishes thus indicating that the particle is driven to accelerate its rotational motion. This result is not surprising because, according to Ref. [16], performing the axial average is equivalent to consider an average particle that is akin to an axially symmetric particle. When the axis around which the average is performed coincides with the direction of \mathbf{k}_1 the result quoted in Ref. [16] follows at once. Moreover, the average of the transverse torque has a deep, nearly vanishing minimum also for values of ϑ_1 that depend on the morphology of the cluster and on the polarization. At these values of ϑ_1 the driving torque $\langle T_z \rangle$, may be small but never vanishing.

It may be interesting to compare the results for cluster C and cluster D reported in Figs. 7 and 8, respectively. Actually both clusters have the same composition but the spheres of cluster C are all of the same volume, whereas those of cluster D all have the same mass. In view of the high density of silver, this implies that the principal moments of inertia of cluster C and D are quite different from each other and, as a result, the values of ϑ_1 at which the average transverse torque becomes nearly vanishing are different. In particular, we note that $\langle T_{\perp} \rangle$ for cluster C nearly vanishes at $\vartheta_1 \approx 100^\circ$ for whatever polarization, whereas $\langle T_{\perp} \rangle$ for cluster D does not show an analogous deep minimum when the incident light is linearly polarized with $\eta = 2$. For both clusters, however, the average driving torque does not vanish neither for incidence along the axis of maximum moment of inertia nor at incidence at which the transverse torque vanishes. We also notice that the driving torque is larger for cluster C that contains more silver and has thus a higher absorptivity.

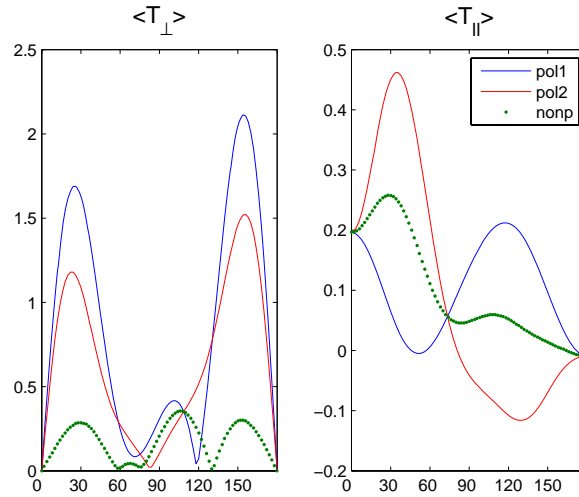


Fig. 6. Same as Fig. 5 for cluster B.

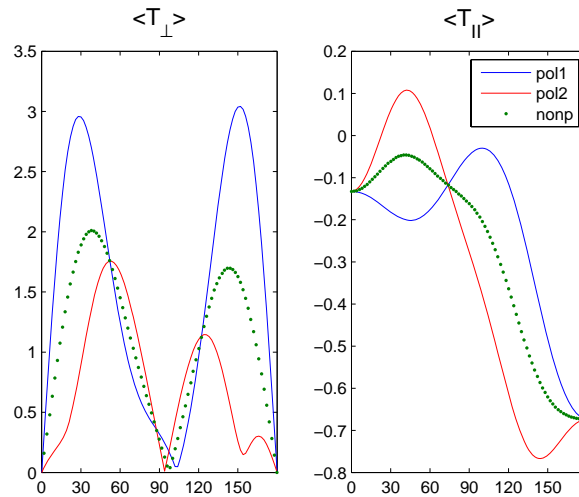


Fig. 7. Same as Fig. 5 for cluster C.

5. Conclusive remarks

The results that we presented in Sects. 3 and 4 show that, at least for the cases we considered, the rotational stability under the affect of the radiation torque may be attained for incidence either parallel or antiparallel to the axis of maximum moment of inertia (z axis). In fact, although the instantaneous transverse torque does not vanish, its axial average does. Thus, provided the initial rotational speed around the z axis is large enough, one could expect that the torque exerted by the incident radiation has the only effect of increasing the angular speed. Of course, this increase of rotational speed cannot go on indefinitely. Nevertheless, we recall that any braking torque has been neglected, and that the presence of braking torques increases the stability of

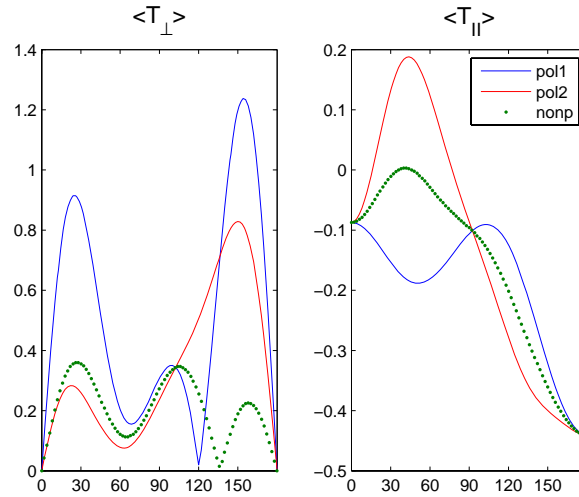


Fig. 8. Same as Fig. 5 for cluster D.

the rotational motion [25]. This problem has been already discussed by Marston and Crichton [12].

We do not pretend that our present results apply to particles of any shape. Nevertheless, the choice of the cluster model may help approximating the shape of particles that are often met in practice. In this respect, let us recall that several particles of astrophysical interest are believed to be composed of aggregated spheres, possibly of different dielectric properties, and that the stability of alignment of the particles is relevant both for the dichroic polarization of the starlight (see, e.g., [29]) and for the occurrence of photochemical reactions both on their surface and in their interior.